A Symmetric and Coercive Finite Volume Scheme for Multiphase Porous Media Flow Problems with Applications in the Oil Industry

L. Agelas — D. A. Di Pietro — R. Masson

Institut Français du Pétrole
1 et 4 avenue Bois Préau
92852 Rueil Malmaison
roland.masson@ifp.fr

ABSTRACT. *Many applications in the oil industry require the efficient simulation of compositional multiphase Darcy flow. Finite volume schemes are often used for this purpose owing to their low computational cost. However, this requires a discretization of the diffusion operator which (i) shows good convergence, stability and complexity properties; (ii) can be used on general polygonal or polyhedral meshes; (iii) can handle heterogeneous and anisotropic diffusion tensors. In this work we introduce a new finite volume scheme which guarantees symmetry, coercivity and convergence on general meshes and for L^∞ diffusion tensors. The robustness of the scheme is numerically assessed.*

KEYWORDS: *finite volumes, anisotropy, general meshes, compositional multiphase Darcy flow*

1. Introduction

Many applications in the oil industry require the simulation of compositional multiphase Darcy flow in heterogeneous porous media: (i) in reservoir modeling, the compositional triphase Darcy flow simulator is a key tool to predict the production of a reservoir and optimize the location of the wells; (ii) in basin modeling, compositional multiphase Darcy flow models are used to simulate the migration of oil and gas phases at geological space and time scales. The flow equations are coupled with models accounting for basin compaction, temperature evolution and for the cracking of the source rock into hydrocarborn components. Such models are used at the exploration stage to predict the location of the reservoirs as well as the quality and quantity of oil trapped therein; (iii) in the study of geological CO_2 storage, the compositional multiphase Darcy model is coupled with the chemical reactions between the aqueous phase

and the minerals. This allows us to model the physical processes occurring during the injection phase and to study the long term stability of the storage.

The numerical simulation of such complex phenomena requires a satisfactory representation of the domain (mesh), an accurate and robust discretization scheme and an efficient solution algorithm. The mesh (i) has to accurately describe complex stratigraphic and structural features such as heterogeneous layers, channels, erosions, and faults and (ii) must be locally refined around the (possibly deviated or multi-branch) wells. These requirements are typically fulfilled by combining structured hexahedric grids with large aspect ratios with locally unstructured meshes. As a consequence, we often have to deal with non-matching or hybrid transition meshes using Voronoi cells or pyramids and prisms.

One of the key ingredients in the numerical scheme is the discretization of the diffusive fluxes in the Darcy law, typically given by $-K\nabla P_\alpha$ where K denotes the permeability tensor and P_α, $\alpha \in \{w, o, g\}$ is the pressure of the water, oil or gas phase. The principal directions of the permeability field follow the directions of the stratigraphic layering, often displaying strong heterogeneities between the layers. Geological features such as channels, faults, conductive faults also lead to strong heterogeneities of the permeability field. Other geological features such as fine scale heterogeneities or extensive fracturing are upscaled up to the flow simulation mesh leading to full, possibly not aligned permeability tensors with large anisotropic ratios. The discretization should therefore be able to handle heterogeneous anisotropic permeabilities on complex meshes, resulting in linear systems solvable by means of preconditioned iterative solvers. The two point approximation of diffusion fluxes currently used in most commercial simulators yields $\mathcal{O}(1)$ consistency errors in the presence of complex geological properties or for general meshes, and the design of an efficient discretization scheme satisfying the above requirements is still a challenge.

In this work, we introduce a new finite volume discretization of diffusive fluxes based on the discrete variational framework developed in [EH 07, EGH 07]. The use of a subgrid allows us to obtain fluxes only between cells sharing a face, as opposed to schemes like the one proposed in [EGH 07], for which fluxes are also defined between pairs of cells whose intersection is of codimension 2. The resulting finite volume scheme is cell-centered, symmetric and coercive on general polygonal or polyhedral meshes and anisotropic heterogeneous media, and can be proved to be convergent even for L^∞ diffusion coefficients under mild shape regularity assumptions. As in [EH 07], the scheme makes it necessary to define a local interpolation operator to approximate the subgrid face unknowns in terms of neighbouring cell unknowns. In order to account for the jumps of the diffusion coefficients at cell boundaries, it is proposed to use an L-type interpolator inspired by [AEMN 07, Aav 05]. Extensive testing on challenging 2D anisotropic diffusion problems shows that the coercivity and symmetry of the scheme provide additional robustness with respect to the skewness of the mesh and the anisotropy of the diffusion tensor.

2. Finite volume discretization of compositional multiphase Darcy flow

2.1. *Compositional multiphase Darcy flow model*

Let us consider a system of n_c components denoted by $\mathcal{C}$, and n_p fluid phases denoted by Φ. For example, for the black oil model we have

$$\mathcal{C} = \{\text{water, heavy hydrocarbon, light hydrocarbon}\}, \quad \Phi = \{\text{aqueous, oil, gas}\}.$$

For the sake of simplicity, we shall assume that all the n_c components can be present in all the n_p fluid phases and that the temperature is fixed. The saturations S_α, $\alpha \in \Phi$, are the volume fractions of the fluid phases, so that $\sum_{\alpha\in\Phi} S_\alpha = 1$. We denote by S the vector $(S_\alpha, \alpha \in \Phi)$. Each fluid phase $\alpha \in \Phi$ is described by its mass compositions $C^\alpha = (C_i^\alpha, i \in \mathcal{C})$, which satisfy $\sum_{i\in\mathcal{C}} C_i^\alpha = 1$. The properties of a given phase $\alpha \in \Phi$ (density, component fugacities, viscosity) depend on its composition C^α and on the reference pressure P, which is assumed to be the same for all phases. The density $\rho_\alpha(C^\alpha, P)$ and the component fugacities $f_{i,\alpha}(C^\alpha, P)$, $i \in \mathcal{C}$, are typically given by an equation of state model. The viscosity will be denoted by $\mu_\alpha(C^\alpha, P)$.

Phase equilibrium calculations will determine the number Φ^p of stable fluid phases present. Observe that Φ^p is a field defined on the computational domain $\Omega \times (0,T)$. The symmetric positive definite permeability tensor field is denoted by K, the porosity field by ϕ and the gravity vector by $\mathbf{g}$. The system of equations accounts for (i) the mass balance of each component in which Darcy's law describes the transport of phases; (ii) the phase equilibrium equations governing the mass transfer of the components between phases; (iii) the pore volume conservation stating that the pore volume is filled by the present fluid phases.

Component mass balance. This expresses the conservation of the mass m_i of each component $i \in \mathcal{C}$. Letting $m_i = \sum_{\alpha\in\Phi^p} \rho_\alpha S_\alpha C_i^\alpha \phi$, and denoting by $\mathbf{V}_\alpha$ the multiphase Darcy velocity, we have

$$\partial_t m_i + \operatorname{div}\Big(\sum_{\alpha\in\Phi^p} C_i^\alpha\, \mathbf{V}_\alpha\Big) = Q_i, \quad \mathbf{V}_\alpha = -\frac{\rho_\alpha\, k_{r_\alpha}}{\mu_\alpha} K\Big(\nabla P_\alpha - \rho_\alpha \mathbf{g}\Big), \qquad [1]$$

where $k_{r_\alpha}(x,S)$ are the relative permeabilities, while $P_\alpha = P + P_{c_\alpha}(x,S)$ denote the phase pressures related to the reference pressure P by the capillarity laws $P_{c_\alpha}(x,S)$.

Phase equilibrium. At each point of the computational domain, it determines the number of present stable fluid phases Φ^p and govern the mass transfer between phases stating the equality of component fugacities:

$$\begin{cases} f_{i,\alpha} = f_{i,\beta}, & \text{for all } \alpha,\beta \in \Phi^p, \\ \sum_{i\in\mathcal{C}} C_i^\alpha = 1, & \text{for all } \alpha \in \Phi^p. \end{cases} \qquad [2]$$

The number of phases Φ^p can be obtained either by flash calculations or by a stability analysis.

Pore volume conservation. This states that the sum of the saturations is one, meaning that the pore volume is saturated with all present phases

$$\sum_{\alpha\in\Phi^p} S_\alpha = 1. \qquad [3]$$

Different formulations of the system of equations [1], [2], [3] have been proposed, which differ by the choice of the set of unknowns and equations. The most popular in the oil industry, introduced in [CTP 98], uses the set of unknowns defined by the pressure P, the compositions $C^\alpha, \alpha \in \Phi^p$, and the saturations $S_\alpha, \alpha \in \Phi^p$, where Φ^p is defined by the flash solution. The set of equations accounts for the mass conservation of the components [1] and the local closure laws [2] and [3], namely

$$\begin{cases} \partial_t\Big(\phi \sum_{\alpha\in\Phi^p} \rho_\alpha(C^\alpha,P)S_\alpha C_i^\alpha\Big) + \operatorname{div}\Big(\sum_{\alpha\in\Phi^p} -\dfrac{\rho_\alpha(C^\alpha,P)\ k_{r_\alpha}(x,S)}{\mu_\alpha(C^\alpha,P)}\ C_i^\alpha \\ \quad K\left[\nabla(P+P_{c_\alpha}(x,S)) - \rho_\alpha(C^\alpha,P)\mathbf{g}\right]\Big) = Q_i, \quad \text{for all } i\in\mathcal{C}, \\ \sum_{\alpha\in\Phi^p} S_\alpha = 1, \\ \sum_{i\in\mathcal{C}} C_i^\alpha = 1, \quad \text{for all } \alpha\in\Phi^p, \\ f_{i,\alpha}(C^\alpha,P) - f_{i,\beta}(C^\beta,P) = 0, \quad \text{for all } i\in\mathcal{C},\ (\alpha,\beta)\in[\Phi^p]^2. \end{cases} \qquad [4]$$

The main advantage of this formulation is to reduce the nonlinearity of the system compared with the mass formulation and to allow arbitrary levels of implicitness in the time integration scheme. This comes at the price of an additional complexity, since different sets of unknowns are used at each point of the computational domain. The system is closed with initial and boundary conditions not discussed in what follows and whose detailed presentation can be found in [CJ 86].

2.2. *Finite Volume Discretization*

Let $\mathcal{D} = (\mathcal{K}, \mathcal{E}, \mathcal{P})$ denote an admissible finite volume discretization of Ω, where:

(i) $\mathcal{K}$ is a finite family of non-empty connex open disjoint subsets of Ω (the "cells") such that $\overline{\Omega} = \cup_{\kappa\in\mathcal{K}}\overline{\kappa}$. For every $\kappa \in \mathcal{K}$, $\partial\kappa = \overline{\kappa} \setminus \kappa$ will denote its boundary and $|\kappa| > 0$ its measure.

(ii) $\mathcal{E}$ is a finite family of disjoint subsets of $\overline{\Omega}$ (the "faces" of the mesh), such that, for all $\sigma \in \mathcal{E}$, σ is a non empty closed subset of a hyperplane of $\mathbb{R}^d$, which has $(d-1)$-dimensional measure $|\sigma| > 0$. We assume that, for all $\kappa \in \mathcal{K}$, there exists a subset $\mathcal{E}_\kappa$ of $\mathcal{E}$ such that $\partial\kappa = \cup_{\sigma\in\mathcal{E}_\kappa}\sigma$ and we let $\mathcal{K}_\sigma = \{\kappa \in \mathcal{K}, \sigma \in \mathcal{E}_\kappa\}$. It is assumed that, for all $\sigma \in \mathcal{E}$, either $\mathcal{K}_\sigma$ has exactly one element and then $\sigma \subset \partial\Omega$ (boundary face $\sigma \in \mathcal{E}_{\rm ext}$) or $\mathcal{K}_\sigma$ has exactly two elements κ, l (interior face $\mathcal{E}_{\rm int} \ni \sigma = \kappa|l$). We denote by x_σ the center of gravity of the face $\sigma \in \mathcal{E}$.

(iii) $\mathcal{P} = (x_\kappa)_{\kappa\in\mathcal{K}}$ is a family of points of Ω indexed by $\mathcal{K}$ ("the cell centers") such that $x_\kappa \in \kappa$. We assume that each cell κ is star-shaped with respect to x_κ.

For all $\kappa \in \mathcal{K}$ and $\sigma \in \mathcal{E}_\kappa$, we denote by $d_{\kappa,\sigma}$ the Euclidean distance between the cell center x_κ and the hyperplane containing the face σ, and by $\mathbf{n}_{\kappa,\sigma}$ the unit vector normal to σ outward to κ. The size of the mesh is defined by $h_\mathcal{K} = \sup_{\kappa\in\mathcal{K}} \text{diameter}(\kappa)$.

The time discretization is defined by the strictly increasing sequence t^n, $n \in \mathbb{N}$. The discrete cell-centered unknowns are identified by the cell subscript κ and the time superscript n: pressure P_κ^n, present fluid phases $\Phi_\kappa^{p,n}$, compositions of the present fluid phases $C_\kappa^{\alpha,n} = \{C_{i,\kappa}^{\alpha,n}, i \in \mathcal{C}\}$, $\alpha \in \Phi_\kappa^{p,n}$, and saturations $S_{\alpha,\kappa}^n, \alpha \in \Phi_\kappa^{p,n}$. The average cell porosity is denoted by ϕ_κ. The cell permeability tensor K_κ, the relative permeability and capillarity laws $k_{r_{\alpha,\kappa}}(S)$ and $P_{c_{\alpha,\kappa}}(S)$ are usually obtained by upscaling of their fine scale description.

For all $i \in \mathcal{C}$ and for all $\kappa \in \mathcal{K}$, let $m_{i,\kappa}^n = \phi_\kappa \sum_{\alpha\in\Phi_\kappa^{p,n}} \rho_\alpha(C_\kappa^{\alpha,n}, P_\kappa^n) S_{\alpha,\kappa}^n C_{i,\kappa}^{\alpha,n}$ be the volumic mass of the component i in the cell κ at time t^n. The discretization accounts for the mass conservation of each component i on each cell κ using fully implicit or semi-implicit Euler time integration schemes

$$\frac{m_{i,\kappa}^{n+1} - m_{i,\kappa}^n}{t^{n+1} - t^n}|\kappa| \; + \sum_{\sigma\in\partial\kappa} \sum_{\alpha\in\{\alpha'\in\Phi \;|\; \alpha'\in\Phi_{\sigma_{\alpha'}}^{p,*}\}} \frac{\rho_\alpha(C_{\sigma_\alpha}^{\alpha,*}, P_{\sigma_\alpha}^*) k_{r_{\alpha,\sigma_\alpha}}(S_{\sigma_\alpha}^*)}{\mu_\alpha(C_{\sigma_\alpha}^{\alpha,*}, P_{\sigma_\alpha}^*)} C_{i,\sigma_\alpha}^{\alpha,*} G_{\alpha,\kappa,\sigma}^{*,n+1} = Q_{i,\kappa}^{n+1}|\kappa|, \quad [5]$$

implicitly coupled with the local closure laws,

$$\begin{cases} \sum_{\alpha\in\Phi_\kappa^{p,n+1}} S_{\alpha,\kappa}^{n+1} = 1, & \\ \sum_{i\in\mathcal{C}} C_{i,\kappa}^{\alpha,n+1} = 1, & \text{for all } \alpha \in \Phi_\kappa^{p,n+1}, \\ f_{i,\alpha}(C_\kappa^{\alpha,n+1}, P_\kappa^{n+1}) - f_{i,\beta}(C_\kappa^{\beta,n+1}, P_\kappa^{n+1}) = 0, & \text{for all } i \in \mathcal{C},\ (\alpha,\beta) \in [\Phi_\kappa^{p,n+1}]^2. \end{cases} \quad [6]$$

In [5], $G_{\alpha,\kappa,\sigma}^{*,n+1}$ is a conservative approximation of the Darcy flux for each phase α at each face σ of the cell κ, i.e.,

$$G_{\alpha,\kappa,\sigma}^{*,n+1} \sim \int_\sigma -K \left[\nabla(P^{n+1} + P_{c_\alpha}(x, S^*)) - \rho_{\alpha,\sigma}^* \mathbf{g}\right] \cdot n_{\kappa,\sigma} \, ds. \quad [7]$$

The approximation is assumed to be conservative, i.e., $G_{\alpha,\kappa,\sigma}^{*,n+1} + G_{\alpha,l,\sigma}^{*,n+1} = 0$ for all face $\sigma = \kappa|l \in \mathcal{E}_{\text{int}}$. The superscript $*$ is equal to $n+1$ for fully implicit schemes and to n for implicit in pressure, explicit in saturations and compositions schemes (impes). The formulation also allows for implicit in pressure and saturations, explicit in composition schemes (impsat) provided that the compositions of the fluid phases are initialized at time n on each cell even for absent phases using, e.g., a negative flash. At each face $\sigma = \kappa|l \in \mathcal{E}_{\text{int}}$, the density $\rho_{\alpha,\sigma}^*$ is an average of the densities in the neighbouring cells κ, and l using, in the case of absent phases at time $*$, an initialization of the compositions at time n.

In order to obtain the stability in space of the discretization scheme, the approximation of the transport terms in (5) at each face $\sigma = \kappa|l \in \mathcal{E}_{\rm int}$ uses the usual "phase" upstream approximation defined for each phase α by

$$\sigma_\alpha = \begin{cases} \kappa, & \text{if } G^{*,n+1}_{\alpha,\kappa,\sigma} > 0, \\ l, & \text{otherwise.} \end{cases} \qquad [8]$$

Discretization [5], [6] is often refered to as the "coupled discretization". This is the most popular approach in the oil industry because it ensures the discrete mass conservation of all components, and it has also proved to be robust in the presence of complex physics. Alternatively, operator splitting time integration schemes solving sequentially for the pressure, saturations and compositions unknowns also exist. If, on the one hand, they allow us to use more advanced discretizations schemes for each equation/unknown separately, on the other hand they introduce splitting errors which may lead to unphysical flow predictions.

2.3. *Discretization of diffusion fluxes*

Darcy fluxes (7) are derived from diffusive fluxes of type $\mathbf{F} = -K\nabla u$, where K is the permeability tensor field, and u is a potential function of the space variable x — in our case $u(x) = P(x)$, $P_{c_\alpha}(x, S(x))$ or $z(x)$. The finite volume discretization of the Darcy fluxes amounts to find a conservative discretization of the diffusion equation

$$\begin{cases} \mathbf{F} = -K\nabla u, & \text{in } \Omega, \\ \text{div}\, \mathbf{F} = Q, & \text{in } \Omega, \\ u = U, & \text{on } \partial\Omega, \end{cases} \qquad [9]$$

using the cell centered unknowns $u_\kappa, \kappa \in \mathcal{K}$. Alternative approaches such as the hybrid finite volume scheme [EGH 07], mimetic finite difference schemes (see e.g. [Bre 05]), or hybrid finite element methods (see e.g. [Kuz 03]) use additional face unknowns which cannot be locally eliminated in terms of the cell unknowns. For multiphase flow applications, however, the computational cost may be unacceptable.

Let $H_\mathcal{K}$ be the function space of piecewise constant functions on each cell $\kappa \in \mathcal{K}$, and let us denote by $v_\mathcal{K}$ the function of $H_\mathcal{K}$ defined by $v_\mathcal{K}(x) = v_\kappa$ on each cell $\kappa \in \mathcal{K}$. The function space $H_\mathcal{K}$ is equipped with the following discrete H^1_0 norm (see [EGH 00]):

$$\|v_\mathcal{K}\|^2_{H_\mathcal{K}} = \sum_{\sigma=\kappa|l\in\mathcal{E}_{\rm int}} |\sigma| \frac{(v_\kappa - v_l)^2}{d_{\kappa,\sigma} + d_{l,\sigma}} + \sum_{\kappa\in\mathcal{K}} \sum_{\sigma\in\mathcal{E}_{\rm ext}\cap\mathcal{E}_\kappa} |\sigma| \frac{(v_\kappa)^2}{d_{\kappa,\sigma}}. \qquad [10]$$

We also define $U_{\mathcal{E}_{\rm ext}} = (U_\sigma = \frac{1}{|\sigma|}\int_\sigma U(x)\, ds,\ \sigma \in \mathcal{E}_{\rm ext})$, and $Q_\kappa = \frac{1}{|\kappa|}\int_\kappa Q(x)\, dx$ for all $\kappa \in \mathcal{K}$. We look for approximations $F_{\kappa,\sigma}(u_\mathcal{K}, U_{\mathcal{E}_{\rm ext}})$ of the normal fluxes $\int_\sigma \mathbf{F}\cdot\mathbf{n}_{\kappa,\sigma}\, ds$ at each face $\sigma \in \mathcal{E}$ satisfying the following properties:

- *Linearity.* $F_{\kappa,\sigma}(u_{\mathcal{K}}, U_{\mathcal{E}_{\rm ext}})$ is a linear function of $u_{\mathcal{K}}$ and $U_{\mathcal{E}_{\rm ext}}$.

- *Conservativity.* $F_{\kappa,\sigma}(u_{\mathcal{K}}, U_{\mathcal{E}_{\rm ext}}) + F_{l,\sigma}(u_{\mathcal{K}}, U_{\mathcal{E}_{\rm ext}}) = 0$ for all $\mathcal{E}_{\rm int} \ni \sigma = \kappa|l$.

- *Consistency.* $|F_{\kappa,\sigma}((\varphi(x_\kappa), \kappa \in \mathcal{K}), (\varphi(x_\sigma), \sigma \in \mathcal{E}_{\rm ext})) - \int_\sigma K(x)\nabla\varphi(x) \cdot \mathbf{n}_{\kappa,\sigma}\, ds| \leq C(\varphi)\, |\sigma|\, h_{\mathcal{K}}$, for all regular functions φ and permeability fields K.

- *Stability.* The norm of the solution $u_{\mathcal{K}}$ should be bounded by the norms of the data f and U. In the framework defined in [EH 07], the coercivity of the bilinear form

$$\mathcal{L}(H_{\mathcal{K}} \times H_{\mathcal{K}}; \mathbb{R}) \ni a_{\mathcal{D}}(u_{\mathcal{K}}, v_{\mathcal{K}}) = \sum_{\sigma \in \mathcal{E}_{\rm int}} F_{\kappa,\sigma}(u_{\mathcal{K}}, 0)(v_\kappa - v_l) + \sum_{\sigma \in \mathcal{E}_{ext}} F_{\kappa,\sigma}(u_{\mathcal{K}}, 0)\, v_\kappa$$

w.r. to norm [10] ensures existence, uniqueness and stability of the solution.

- *Convergence.* the unique discrete solution $u_{\mathcal{K}}$ of

$$\sum_{\sigma \in \mathcal{E}_\kappa} F_{\kappa,\sigma}(u_{\mathcal{K}}, U_{\mathcal{E}_{\rm ext}}) = |\kappa|\, Q_\kappa, \qquad \text{for all } \kappa \in \mathcal{K}, \tag{11}$$

should converge to u in $L^2(\Omega)$ as $h_{\mathcal{K}} \to 0$. The convergence should hold on general meshes with usual shape regularity assumptions, and for L^∞ anisotropic heterogeneous permeability fields with eigenvalues uniformly bounded from below and above.

Problem [11] can be recast into the equivalent variational formulation: find $u_\kappa \in H_{\mathcal{K}}$ such that

$$a_{\mathcal{D}}(u_{\mathcal{K}}, v_{\mathcal{K}}) = \int_\kappa Q_\kappa\, v_{\mathcal{K}} + b_{\mathcal{D}}(v_{\mathcal{K}}), \quad \text{for all } v_{\mathcal{K}} \in H_{\mathcal{K}}, \tag{12}$$

where the linear form $b_{\mathcal{K}}$ is used to enforce boundary conditions. We require the following additional properties to be satisfied: (i) the bilinear form $a_{\mathcal{D}}$ should be symmetric. This condition is so far the only way to obtain the coercivity of the scheme on general meshes; (ii) the discretization scheme should provide fairly accurate solutions for cellwise constant diffusion coefficients even in the case of large jumps and rough grids frequently encountered in oil industry applications.

The most popular cell centered approaches in the oil industry are the so called multipoint flux approximation (MPFA) schemes. The classical MPFA O method [Aav 02, Edw 02, Gun 98] provides local explicit formulæ for the fluxes, it is exact for piecewise linear solutions on general unstructured meshes, and allows cellwise discontinuous, anisotropic diffusion coefficients. On the other hand, however, it may encounter stability problems due to the lack of coercivity on very distorted meshes or in the presence of strong anisotropies (see [Kla 06, Aav 07, AM 07]). More recent MPFA methods such as the L method [AEMN 07, Aav 05] have more compact stencils and increased stability properties. However, the coercivity and convergence of the L method, which still have to be theoretically analysed, are likely to be mesh and anisotropy dependent due to the lack of symmetry in the construction. Symmetric and coercive versions of the O method have also been proposed in [LeP 05, LSY 05]. Although convergence was proved on simplicial meshes and smoothed quadrangular

or hexahedral grids, they do not apply or converge on general polygonal or polyhedral meshes.

To our knowledge, the only cell centered finite volume scheme which is symmetric, coercive and convergent on general meshes is the one introduced in [EH 07]. The above-mentioned scheme is based on a hybrid discrete variational formulation using cell and face unknowns as well as local linear interpolation operators to eliminate the face unknowns in terms of the neighbouring cell unknowns. In this approach, the fluxes have to be defined in a wider sense, since they connect pairs of cells whose intersection is a set of codimension 2. In the next section, a new method based on the same variational framework is proposed (i) for which fluxes are defined in the usual sense; (ii) which provides a cell centered symmetric, coercive and convergent discretization on general polygonal and polyhedral meshes; (iii) which allows strong heterogeneity and anisotropy.

3. A symmetric, coercive, convergent cell centered finite volume scheme on general polygonal and polyhedral meshes

The scheme discussed in this section is based on the framework developed in [EH 07, EGH 07] using a hybrid formulation with cell and face unknowns u_κ, $\kappa \in \mathcal{K}$, and u_σ, $\sigma \in \mathcal{E}$. The discrete gradient reconstruction is piecewise constant on a subgrid, and the face unknowns u_σ, $\sigma \in \mathcal{E}_{\rm int}$ are locally eliminated solving a flux continuity equation.

Define the discrete function space $H_{\mathcal{K},\mathcal{E}} = H_\mathcal{K} \times \{(v_\sigma)_{\sigma\in\mathcal{E}};\ v_\sigma \in \mathbb{R} \text{ for all } \sigma \in \mathcal{E}\}$, and denote by $v_{\mathcal{K},\mathcal{E}} = (v_\mathcal{K}, v_\mathcal{E})$ the generic element of $H_{\mathcal{K},\mathcal{E}}$. The restrictions of $v_\mathcal{E}$ to internal and boundary faces will be denoted by $v_{\mathcal{E}_{\rm int}}$ and by $v_{\mathcal{E}_{\rm ext}}$ respectively. The function space $H_{\mathcal{K},\mathcal{E}}$ is equipped with the discrete scalar product

$$\langle v_{\mathcal{K},\mathcal{E}}, w_{\mathcal{K},\mathcal{E}}\rangle_{H_{\mathcal{K},\mathcal{E}}} = \sum_{\kappa\in\mathcal{K}}\sum_{\sigma\in\mathcal{E}_\kappa} \frac{|\sigma|}{d_{\kappa,\sigma}}(v_\kappa - v_\sigma)(w_\kappa - w_\sigma).$$

The associated seminorm $\|\cdot\|_{H_{\mathcal{K},\mathcal{E}}}$ satisfies the following property:

$$\|v_\mathcal{K}\|_{H_\mathcal{K}} = \min_{v_{\mathcal{E}_{\rm ext}}=0} \|v_{\mathcal{K},\mathcal{E}}\|_{H_{\mathcal{K},\mathcal{E}}}.$$

The subgrid of each cell κ of the mesh is defined by the set of pyramids $\{\kappa_\sigma\}_{\sigma\in\mathcal{E}_\kappa}$, of d-dimensional measure $|\kappa_\sigma|$, joining the face σ to the cell center x_κ. We denote by $\mathcal{E}_{\kappa_\sigma}$ the set of $(d-1)$-dimensional faces e of κ_σ interior to the cell κ such that $\partial\kappa_\sigma = \bigcup_{e\in\mathcal{E}_{\kappa_\sigma}} e \cup \sigma$. The $(d-1)$-dimensional measure of e is denoted by $|e|$, its barycenter by x_e, and its unit normal vector outward to κ_σ by $\mathbf{n}_{\kappa_\sigma,e}$. The distance from the barycenter of κ_σ to $f \in \mathcal{E}_{\kappa_\sigma} \cup \{\sigma\}$ is denoted by $d_{\kappa_\sigma,f}$. The following property holds for any polygonal or polyhedral cell κ_σ:

$$\frac{1}{|\kappa_\sigma|}\Big(|\sigma|\mathbf{n}_{\kappa,\sigma}(x_\sigma - x_\kappa)^t + \sum_{e\in\mathcal{E}_{\kappa_\sigma}} |e|\mathbf{n}_{\kappa_\sigma,e}\,(x_e - x_\kappa)^t\Big) = I, \qquad [13]$$

Using (13), a consistent discrete gradient can be defined on each subcell κ_σ by

$$(\nabla v_{\mathcal{K},\mathcal{E}})_{\kappa_\sigma} = \frac{1}{|\kappa_\sigma|}\Big[|\sigma|(u_\sigma - u_\kappa)\mathbf{n}_{\kappa,\sigma} + \sum_{e\in\mathcal{E}_{\kappa_\sigma}} |e|\Big(\Pi_e(v_\mathcal{K}, v_{\mathcal{E}_{\rm ext}}) - v_\kappa\Big)\mathbf{n}_{\kappa_\sigma,e}\Big].$$

The operator Π_e is a linear interpolation operator which uses the cell unknowns v_l for cells l sharing a face with the cell κ, $e \in \kappa_\sigma$ and, possibly, local boundary face unknowns. It is consistent in the following sense: for all smooth functions φ, there exists a constant $C(\varphi)$ depending only on φ such that

$$|\Pi_e((\varphi(x_\kappa), \kappa\in\mathcal{K}), (\varphi(x_\sigma), \sigma\in\mathcal{E}_{\rm ext})) - \varphi(x_e)| \le C(\varphi)\ h_\mathcal{K}^2. \qquad [14]$$

Consider the following bilinear form on $H_{\mathcal{K},\mathcal{E}} \times H_{\mathcal{K},\mathcal{E}}$:

$$\begin{aligned} a_\mathcal{D}(u_{\mathcal{K},\mathcal{E}}, v_{\mathcal{K},,\mathcal{E}}) = &\sum_{\kappa\in\mathcal{K}}\sum_{\sigma\in\mathcal{E}_\kappa}\Big[|\kappa_\sigma|(\nabla u_{\mathcal{K},\mathcal{E}})_{\kappa_\sigma} K_\kappa (\nabla v_{\mathcal{K},\mathcal{E}})_{\kappa_\sigma} \\ &+ \alpha_{\kappa,\sigma}\sum_{f\in\mathcal{E}_{\kappa_\sigma}\cup\{\sigma\}}\frac{|\sigma|}{d_{\kappa_\sigma,f}} R_{\kappa_\sigma,f}(u_{\mathcal{K},\mathcal{E}}) R_{\kappa_\sigma,f}(v_{\mathcal{K},\mathcal{E}})\Big], \end{aligned} \qquad [15]$$

where $\alpha_{\kappa,\sigma}$ is a positive real and the residual functions are defined as follows: for all $\sigma\in\mathcal{E}_\kappa, \kappa\in\mathcal{K}$

$$\begin{cases} R_{\kappa_\sigma,e}(v_{\mathcal{K},\mathcal{E}}) = \Pi_e(v_{\mathcal{K},\mathcal{E}_{\rm ext}}) - v_\kappa - (x_\sigma - x_\kappa)^t(\nabla v_{\mathcal{K},\mathcal{E}})_{\kappa_\sigma}, & \text{for all } e\in\mathcal{E}_{\kappa_\sigma},\\ R_{\kappa_\sigma,\sigma}(v_{\mathcal{K},\mathcal{E}}) = v_\sigma - v_\kappa - (x_\sigma - x_\kappa)^t(\nabla v_{\mathcal{K},\mathcal{E}})_{\kappa_\sigma}. \end{cases}$$

The stabilization term involving the residuals allows us to prove the coercivity of $a_\mathcal{D}$ with respect to the $\|\cdot\|_{H_{\mathcal{K},\mathcal{E}}}$ seminorm under the usual shape regularity assumptions. In discrete variational form the problem reads: find $u_{\mathcal{K},\mathcal{E}}\in H_{\mathcal{K},\mathcal{E}}$ such that $u_{\mathcal{E}_{\rm ext}} = U_{\mathcal{E}_{\rm ext}}$ and, for all $v_{\mathcal{K},\mathcal{E}}\in H^0_{\mathcal{K},\mathcal{E}}$,

$$a_\mathcal{D}(u_{\mathcal{K},\mathcal{E}}, v_{\mathcal{K},\mathcal{E}}) = \int_\Omega Q\ v_\mathcal{K}\ dx,$$

where $H^0_{\mathcal{K},\mathcal{E}}$ is the subspace of $H_{\mathcal{K},\mathcal{E}}$ with vanishing boundary face values. The above formulation is equivalent to the following hybrid finite volume scheme

$$\begin{cases} \sum_{\sigma\in\mathcal{E}_\kappa} F_{\kappa,\sigma}(u_\mathcal{K}, u_\mathcal{E}) = |\kappa| Q_\kappa, & \text{for all } \kappa\in\mathcal{K},\\ F_{\kappa,\sigma}(u_\mathcal{K}, u_\mathcal{E}) + F_{l,\sigma}(u_\mathcal{K}, u_\mathcal{E}) = 0, & \text{for all } \sigma = \kappa|l\in\mathcal{E}_{\rm int},\\ u_\sigma = U_\sigma, & \text{for all } \sigma\in\mathcal{E}_{\rm ext}, \end{cases} \qquad [16]$$

where the fluxes are defined by

$$a_\mathcal{D}(u_{\mathcal{K},\mathcal{E}}, v_{\mathcal{K},\mathcal{E}}) = \sum_{\kappa\in\mathcal{K}}\sum_{\sigma\in\mathcal{E}_\kappa} F_{\kappa,\sigma}(u_\mathcal{K}, u_\mathcal{E})(v_\kappa - v_\sigma), \quad \forall v_{\mathcal{K},\mathcal{E}}\in H^0_{\mathcal{K},\mathcal{E}}.$$

The second equation of [16] actually involves the only face value u_σ, which can therefore be expressed in terms of cell unknowns leading to a cell centered scheme.

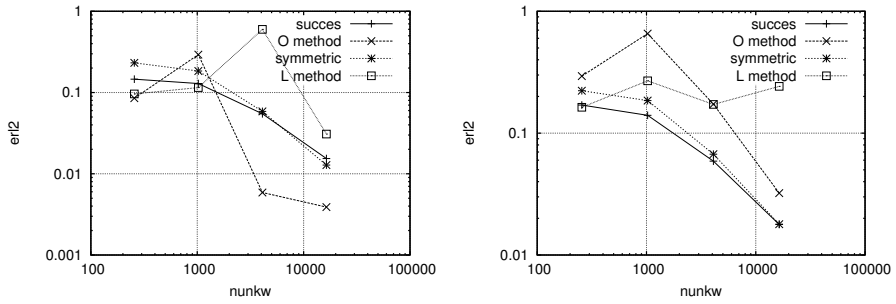

(a) $\delta = 10$ (b) $\delta = 10^2$

Figure 1. *Convergence results for Test case 1 (`erl2` and `nunkw` denote, respectively, the discrete L^2-error and the number of unknowns).*

To complete the description of the method, it only remains to choose the interpolation operator Π_e. A possible choice is the second order interpolation operator proposed in [EH 07], which was designed to reproduce linear functions. However, oil industry applications require that the interpolation operators Π_e be able to handle cellwise constant discontinuous diffusion tensors. To this purpose, we propose here to use the L-type interpolation operator defined in [AEMN 07, Aav 05]. This interpolation operator depends on the diffusion tensor and does not satisfy property (14) for discontinuous diffusion coefficients but it guarantees that our finite volume scheme will reproduce cellwise linear solutions for cellwise constant diffusion tensors.

By construction, the resulting scheme is symmetric and coercive on general meshes. Convergence can be proved under mild shape regularity assumptions and for continuous diffusion tensors if the L-type interpolator is used, and for L^∞ diffusion tensors when the second order interpolation operator of [EH 07] is selected. However, this increased robustness comes at the price of larger flux stencils. Indeed, when topologically Cartesian meshes are used, the stencil of the scheme is composed of 21 cells in two dimensions and of 81 cells in three dimensions.

4. Numerical examples on single-phase flow problems

The objective of this section is to assess the performance of the method discussed in section 3 (henceforth refered to as "Symmetric") on challenging diffusion problems combining mild or strong anisotropy and distorted meshes. For the sake of completeness, we shall compare the results against (i) the method of [EH 07] combined with the L type interpolation operator and refered to as "SUCCES", (ii) the MPFA O method of [Aav 02] and (iii) the MPFA L method of [Aav 07].

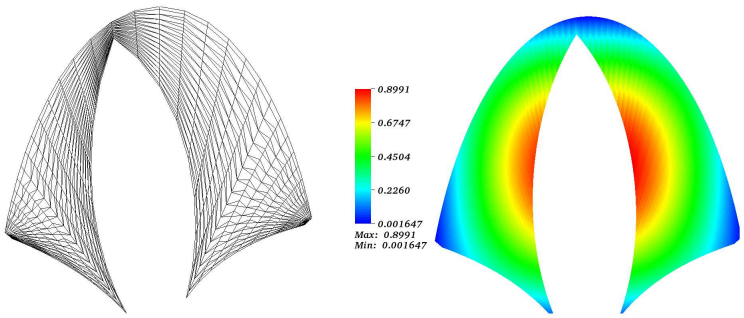

(a) Mesh 2 (b) Solution on mesh 2

Figure 2. *Mesh 2 of Test case 1 and the solution obtained by the Symmetric scheme*

	L scheme		O scheme	
i	umin	umax	umin	umax
1	$1.91e-02$	$1.03e+00$	$1.79e-02$	$1.14e+00$
2	$7.87e-03$	$9.42e-01$	$-3.24e-01$	$1.52e+00$
3	$-1.80e+00$	$2.60e+00$	$3.53e-03$	$9.17e-01$
4	$1.66e-03$	$8.99e-01$	$1.66e-03$	$8.98e-01$
	SUCCES		Symmetric	
i	umin	umax	umin	umax
1	$2.37e-02$	$1.00e+00$	$1.93e-02$	$1.14e+00$
2	$8.23e-03$	$9.77e-01$	$7.75e-03$	$1.08e+00$
3	$3.59e-03$	$9.19e-01$	$3.51e-03$	$9.28e-01$
4	$1.67e-03$	$8.97e-01$	$1.65e-03$	$8.99e-01$

Table 1. *Minimum and maximum solution values for Test case 1 ($\delta = 10$).*

4.1. *Test case 1*

We solve the anisotropic diffusion test case introduced in [LeP 05] on a family of highly-skewed mesh of the domain $\Omega \subset [0,1]^2$ containing both triangular and quadrangular elements. Here and in the following test cases, the meshes are indexed by $i \in \mathbb{N}$ starting from the coarsest mesh $i = 1$. The mesh 2 of Test case 1 is plotted

	L scheme		O scheme	
i	umin	umax	umin	umax
1	$1.91e-02$	$1.04e+00$	$-3.58e-01$	$1.81e+00$
2	$-4.24e-01$	$1.72e+00$	$-3.21e+00$	$2.97e+00$
3	$-9.81e-03$	$1.19e+00$	$-5.95e-01$	$1.11e+00$
4	$-5.28e-01$	$1.88e+00$	$-2.01e-01$	$9.05e-01$
	SUCCES		Symmetric	
1	$2.40e-02$	$1.00e+00$	$1.98e-02$	$1.16e+00$
2	$8.19e-03$	$9.77e-01$	$7.65e-03$	$1.11e+00$
3	$3.58e-03$	$9.20e-01$	$3.48e-03$	$9.35e-01$
4	$1.67e-03$	$8.98e-01$	$1.65e-03$	$8.99e-01$

Table 2. *Minimum and maximum solution values for Test case 1 ($\delta = 10^2$).*

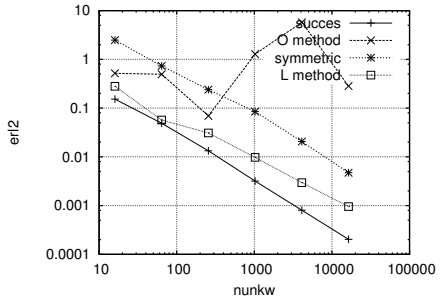

Figure 3. *Convergence results for Test case 2 (`erl2` and `nunkw` denote, respectively, the discrete L^2-error and the number of unknowns).*

in Figure 2 together with the solution obtained with the Symmetric scheme. The exact solution and the expression for the permeability coefficient are given below:

$$u = \sin(\pi x)\sin(\pi y), \quad K = \frac{1}{x^2+y^2}\begin{bmatrix} \delta x^2 + y^2 & (\delta-1)xy \\ (\delta-1)xy & x^2 + \delta y^2 \end{bmatrix}. \qquad [17]$$

Here and in what follows, we shall understand that Dirichlet boundary conditions are given on each boundary edge $\sigma \in \mathcal{E}_{\rm int}$ by $u(x_\sigma)$, and that the forcing term is equal to $-\nabla\cdot(K\nabla u)$. The parameter δ is in fact the ratio between the minimum and the maximum eigenvalue of K. In Figure 4 we compare the four schemes in terms of the discrete L^2-error for $\delta = 10$ and $\delta = 10^2$.

In this and in the following test cases the exact solution is chosen in such a way that its extrema on the unit square domain are $u_{\min} = 0$ and $u_{\max} = 1$ respectively. The extrema of the discrete solution are listed in Tables 4 and 4. When such values fall beyond the interval $(0, 1)$, a violation of the maximum principle occurs.

	L scheme		O scheme	
i	umin	umax	umin	umax
1	$1.59e-02$	$1.03e+00$	$7.55e-3$	$1.70e+00$
2	$3.50e-03$	$9.88e-01$	$-1.05e-01$	$1.49e+00$
3	$1.07e-04$	$1.01e+00$	$5.48e-04$	$1.20e+00$
4	$5.70e-04$	$1.00e+00$	$-2.98e+00$	$4.95e+00$
5	$-1.71e-04$	$1.00e+00$	$-1.70e+01$	$3.54e+01$
6	$-7.71e-05$	$1.00e-00$	$-1.80e+00$	$2.30e+00$
	SUCCES		Symmetric	
1	$4.33e-02$	$8.98e-01$	$-8.23e-01$	$2.84e+00$
2	$1.22e-02$	$9.63e-01$	$-1.34e-01$	$1.93e+00$
3	$6.40e-03$	$9.84e-01$	$-1.47e-02$	$1.29e+00$
4	$5.23e-04$	$9.96e-01$	$4.39e-04$	$1.11e+00$
5	$1.30e-04$	$1.00e-00$	$8.82e-05$	$1.04e+00$
6	$5.77e-05$	$1.00e-00$	$7.07e-05$	$1.00e+00$

Table 3. *Minimum and maximum solution values for Test case 2.*

	L scheme		O scheme	
i	umin	umax	umin	umax
1	$9.95e-03$	$1.00+00$	$8.70e-03$	$9.73e-01$
2	$2.33e-03$	$9.66e-01$	$2.25e-03$	$9.91e-01$
3	$1.06e-03$	$9.79e-01$	$1.01e-03$	$9.96e-01$
4	$6.11e-04$	$9.86e-01$	$5.71e-04$	$9.98e-01$
	SUCCES		Symmetric	
1	$7.82e-03$	$8.54e-01$	$2.14e-03$	$9.84e-01$
2	$1.93e-03$	$8.95e-01$	$6.47e-04$	$9.98e-01$
3	$9.19e-04$	$9.33e-01$	$2.74e-04$	$1.00e-00$
4	$5.43e-04$	$9.55e-01$	$1.49e-04$	$1.00e+00$

Table 4. *Minimum and maximum solution values for test 3, mesh family 4.1.*

4.2. *Test case 2*

In this test case we combine a randomly distorted mesh with a highly-anisotropic uniform permeability tensor. The exact solution and the permeability coefficient are chosen as follows:

$$u = \sin(\pi x)\sin(\pi y), \quad K = \begin{bmatrix} 10^3 & 0 \\ 0 & 1 \end{bmatrix}.$$

In Figure 3 we compare the four schemes in terms of the discrete L^2-error. The extrema of the discrete solution are listed in Table 4.1.

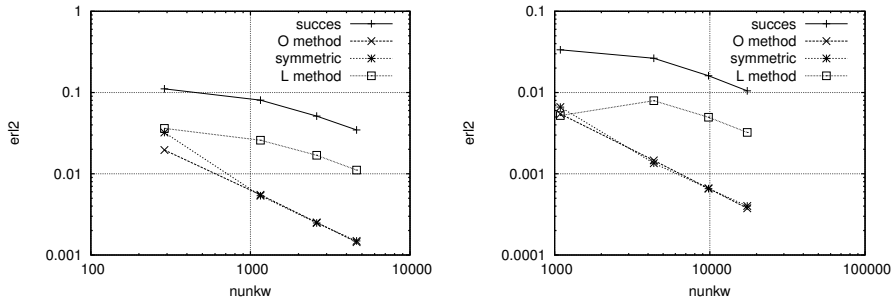

(a) Mesh family 4.1 (b) Mesh family 4.2

Figure 4. *Convergence results for Test case 3 (`erl2` and `nunkw` denote, respectively, the discrete L^2-error and the number of unknowns).*

	L scheme		O scheme	
i	umin	umax	umin	umax
1	$2.73e-03$	$9.99e-01$	$2.45e-03$	$9.92e-01$
2	$6.73e-04$	$9.86e-01$	$6.13e-04$	$9.97e-01$
3	$3.01e-04$	$9.92e-01$	$2.72e-04$	$9.99e-01$
4	$1.70e-04$	$9.95e-01$	$1.53e-04$	$9.99e-01$
	SUCCES		Symmetric	
1	$2.45e-03$	$9.52e-01$	$7.16e-04$	$9.93e-01$
2	$6.19e-04$	$9.60e-01$	$1.61e-04$	$9.99e-01$
3	$2.81e-04$	$9.75e-01$	$6.75e-05$	$1.00e-00$
4	$1.60e-04$	$9.83e-01$	$3.67e-05$	$1.00e-00$

Table 5. *Minimum and maximum solution values for Test case 3, mesh family 4.2.*

4.3. *Test case 3*

In this test case we solve a problem with moderate anisotropy on the two families of Kershaw meshes provided for the FVCA5 benchmark labelled 4.1 and 4.2 (see [HH 07]) respectively. The exact solution and the permeability coefficient are chosen as follows:

$$u = 16x(1-x)y(1-y), \quad K = \begin{bmatrix} 1.5 & 0.5 \\ 0.5 & 1.5 \end{bmatrix}.$$

In Figure 4 we compare the four schemes in terms of the discrete L^2-error. The extrema of the discrete solution are listed in Tables 4.2 and 4.2.

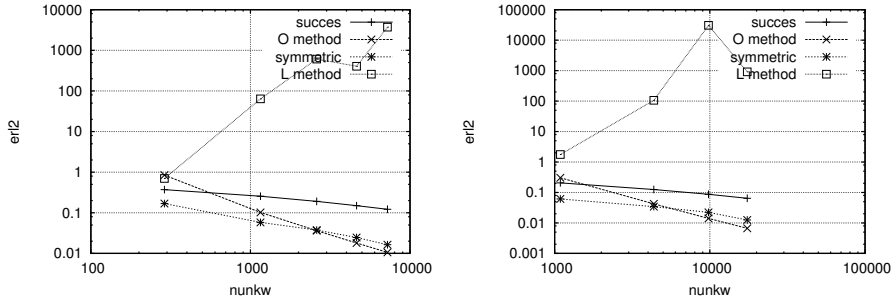

(a) Mesh family 4.1

(b) Mesh family 4.2

Figure 5. *Convergence results for Test case 4 (`erl2` an `nunkw` denote, respectively, the discrete L^2-error and the number of unknowns).*

	L scheme		O scheme	
i	umin	umax	umin	umax
1	$-8.20e-01$	$1.58e+00$	$-8.58e-02$	$2.39e+00$
2	$-3.56e+02$	$3.35e+02$	$-1.76e-02$	$1.14e+00$
3	$-5.70e+03$	$5.96e+03$	$-9.27e-03$	$1.04e+00$
4	$-3.47e+03$	$3.52e+03$	$-5.97e-03$	$1.02e+00$
	SUCCES		Symmetric	
1	$-3.22e-03$	$6.08e-01$	$-1.01e+00$	$9.97e-01$
2	$-5.24e-03$	$7.26e-01$	$-2.92e-01$	$1.03e+00$
3	$-9.74e-03$	$7.91e-01$	$-1.38e-01$	$1.02e+00$
4	$-1.07e-02$	$8.34e-01$	$-7.76e-02$	$1.01e+00$

Table 6. *Minimum and maximum solution values for Test case 4, mesh family 4.1.*

	L scheme		O scheme	
i	umin	umax	umin	umax
1	$-3.87e+00$	$5.44e+00$	$-3.15e-02$	$1.48e+00$
2	$-1.26e+03$	$1.26e+03$	$-6.58e-03$	$1.06e+00$
3	$-4.54e+05$	$4.73e+05$	$-3.32e-03$	$1.02e+00$
4	$-1.68e+04$	$1.71e+04$	$-2.00e-03$	$1.01e+00$
	SUCCES		Symmetric	
1	$-3.82e-04$	$7.93e-01$	$-3.51e-01$	$9.98e-01$
2	$-2.83e-04$	$8.55e-01$	$-8.15e-02$	$9.95e-01$
3	$-1.44e-04$	$8.96e-01$	$-3.65e-02$	$1.00e+00$
4	$-7.96e-05$	$9.22e-01$	$-2.06e-02$	$1.00e+00$

Table 7. *Minimum and maximum solution values for Test case 4, mesh family 4.2.*

4.4. *Test case 4*

We consider again the anisotropic test case [17] with $\delta = 10^3$ and we solve it on the two Kershaw mesh families used in §4.3. In Figure 5 we compare the four schemes in terms of the discrete L^2-error. The extrema of the discrete solution are listed in Tables 4.3 and 4.3.

5. Conclusion

As expected, both the symmetric and coercive schemes display an increased robustness in terms of convergence behavior with respect to the distorsion of the mesh and the anisotropy of the diffusion tensor. In terms of monotonicity, the comparison is less clear, since all test cases are beyond the monotonicity zone. Nevertheless, both the symmetric and the SUCCES schemes provide good results compared with the L and O methods. However, these increased convergence properties on difficult anisotropic problems are obtained at the expense of larger scheme and flux stencils, and additional work is still needed done to find more compact finite volume schemes ensuring such robust convergence properties.

6. Acknowledgements

The authors would like to thank Robert Eymard (University Paris-Est) for his helpful comments during the elaboration of this work, as well as the organizers of the FVCA5 benchmark session Raphaele Herbin and Florence Hubert for providing a part of the test cases presented in this article. We are also grateful to Sissel Mundal (CIPR) for the fruitful discussions and her implementation of the L method during her stay at IFP.

7. References

[Aav 02] AAVATSMARK I., "An introduction to multipoint flux approximations for quadrilateral grids", *Computational Geosciences* 6, 2002, p. 405-432.

[Aav 05] AAVATSMARK I. , EIGESTAD G.T. , HEIMSUND B.O. , MALLISON B.T. , NORDBOTTEN J.M. "A new Finite Volume Approach to Efficient Discretization on Challenging Grids", *Proc. SPE 106435, Houston, 2005*.

[Aav 07] AAVATSMARK I. , EIGESTAD G.T. , KLAUSEN R.A. , WHEELER M.F. , YOTOV I., " Convergence of a symmetric MPFA method on quadrilateral grids", *Computational Geosciences*, 2007.

[AEMN 07] AAVATSMARK I. , EIGESTAD G.T. , MALLISON B.T. , NORDBOTTEN J.M. "A compact multipoint flux approximation method with improved robustness", *Computational Geosciences, accepted for publication 2007*.

[AE 08] AGELAS L. , EYMARD R., "A symmetric finite volume scheme for the approximation of the diffusion equation on general meshes ", *Numerishe Mathematics*, submitted, 2008.

[AM 07] AGELAS L. , MASSON R., "Convergence of the Finite Volume MPFA O Scheme for Heterogeneous Anisotropic Diffusion Problems on General Meshes", *Comptes rendus Mathématiques de l'Académie des Sciences*, submitted, 2007.

[Bre 05] BREZZI F. , LIPNIKOV K. , SIMONCINI V., "A family of mimetic finite difference methods on polygonal and polyhedral meshes", *Mathematical Models and Methods in Applied Sciences*, vol. 15, 10, 2005, p. 1533-1552.

[CJ 86] CHAVENT G. , JAFFRÉ J. "Mathematical Models and Finite Elements for Reservoir Simulation", *Studies in Mathematics and its applications, J.L. Lions, G. Papanicolaou, H. fujita, H.B. Keller editors, vol. 17, North Holland, Elsevier, 1986*.

[CTP 98] COATS K.H. , THOMAS L.K. , PIERSON R.G. "Compositional and Black Oil Reservoir Simulation", *SPE Reservoir Evaluation and Engineering 50990, 1998*.

[Edw 02] EDWARDS M.G., "Unstructured control-volume distributed full tensor finite volume schemes with flow based grids", *Computational Geosciences*, 6, 2002 p. 433-452.

[EGH 00] EYMARD R. , GALLOUËT T. , HERBIN R. "The Finite Volume Method", *Handbook of Numerical Analysis, P.G. Ciarlet, J.L. Lions editors, Elsevier,* **7***, 2000 p. 715-1022*.

[EH 07] EYMARD R. , HERBIN R., "A new colocated finite volume scheme for the incompressible Navier-Stokes equations on general non matching grids", *Comptes rendus Mathématiques de l'Académie des Sciences*, 344(10), p. 659-662, 2007.

[EGH 07] EYMARD R. , GALLOUËT T., HERBIN R., "A new finite volume scheme for anisotropic diffusion problems on general grids: convergence analysis", *Comptes rendus Mathématiques de l'Académie des Sciences*, 344,6, 2007, p. 403-406.

[Gun 98] GUNASEKERA D. , CHILDS P. , HERRING J. , COX J., "A multi-point flux discretization scheme for general polyhedral grids", *Proc. SPE 6th international Oil and Gas Conference and Exhibition, China*, SPE 48855 nov. 1998.

[HH 07] HERBIN R. , HUBERT F., "Benchmark session: finite volume schemes on general grids for anisotropic and heterogeneous diffusion problems, http://wwww.latp.univ-mrs.fr/fvca5/ ", *Finite Volume for Complex Applications Congress*, june 2007.

[Kla 06] KLAUSEN R.A. , WINTHER R., "Robust convergence of multi point flux approximation on rough grids", *Numer. Math.*, 104, 3, 2006, p. 317-337.

[Kuz 03] KUZNETSOV Y. , REPIN S., "New Mixed Finite Element Method on Polygonal and Polyhedral Meshes", *Journal of Numerical and Mathematical Modelling*, vol. 18,3, 2003 p. 261-278.

[LeP 05] LE POTIER C., "Finite volume scheme for highly anisotropic diffusion operators on unstructured meshes", *Comptes rendus Mathématiques de l'Académie des Sciences*, 340, 2005.

[LSY 05] LIPNIKOV K. , SHASHKOV M. , YOTOV I., "Local flux mimetic finite difference methods", *Technical Report Los Alamos National Laboratory* LA-UR-05-8364, 2005.